Design and Synthesis of a FlAsH-Type Mg^{2+} Fluorescent Probe for Specific Protein Labeling

Tomohiko Fujii,[†,‡,⊥] Yutaka Shindo,[†,⊥] Kohji Hotta,[†] Daniel Citterio,[§] Shigeru Nishiyama,[∥] Koji Suzuki,[§] and Kotaro Oka*,[†]

[†]Department of Biosciences and Informatics, [§]Department of Applied Chemistry, and [∥]Department of Chemistry, Faculty of Science and TechnologyKeio University, 3-14-1 Hiyoshi, Kohoku-ku, Yokohama 223-8522, Japan
[‡]Graduate School of Medicine, University of Tokyo, 7-3-1 Hong, Bunkyo-ku, Tokyo 113-0033, Japan

Ⓢ *Supporting Information*

ABSTRACT: Although the magnesium ion (Mg^{2+}) is one of the most abundant divalent cations in cells and is known to play critical roles in many physiological processes, its mobilization and underlying mechanisms are still unknown. Here, we describe a novel fluorescent Mg^{2+} probe, "KMG-104-AsH", composed of a highly selective fluorescent Mg^{2+} probe, "KMG-104", and a fluorescence-recoverable probe, "FlAsH", bound specifically to a tetracysteine peptide tag (TCtag), which can be genetically incorporated into any protein. This probe was developed for molecular imaging of local changes in intracellular Mg^{2+} concentration. KMG-104-AsH was synthesized, and its optical properties were investigated in solution. The fluorescence intensity of KMG-104-AsH (at $\lambda_{em/max}$ = 540 nm) increases by more than 10-fold by binding to both the TCtag peptide and Mg^{2+}, and the probe is highly selective for Mg^{2+} ($K_{d/Mg}$ = 1.7 mM, $K_{d/Ca} \gg$ 100 mM). Application of the probe for imaging of Mg^{2+} in HeLa cells showed that this FlAsH-type Mg^{2+} sensing probe is membrane-permeable and binds specifically to tagged proteins, such as TCtag-actin and mKeima-TCtag targeted to the cytoplasm and the mitochondrial intermembrane space. KMG-104-AsH bound to TCtag responded to an increase in intracellular Mg^{2+} concentration caused by the release of Mg^{2+} from mitochondria induced by FCCP, a protonophore that eliminates the inner membrane potential of mitochondria. This probe is expected to be a strong tool for elucidating the dynamics and mechanisms of intracellular localization of Mg^{2+}.
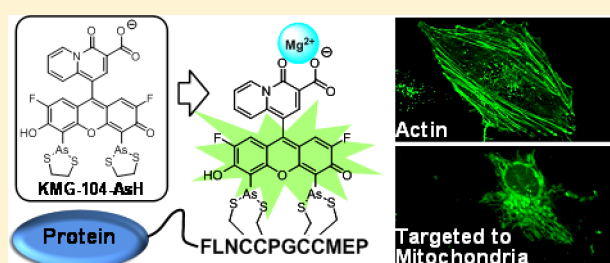
■ INTRODUCTION

The magnesium ion (Mg^{2+}) is an abundant divalent cation in cells. Intracellular Mg^{2+} plays critical roles in many physiological processes including the regulation of hundreds of enzymes, activities of membrane proteins including ion channels,[1−4] and the activity of enzymes involved in ATP synthesis in mitochondria.[5] Mg^{2+} is also involved in several disorders. A decrease in Mg^{2+} concentration and abnormal metabolic processing of intracellular Mg^{2+} have been implicated in the development of migraines, diabetes, hypertension, and Parkinson's disease.[6−10] Furthermore, Mg^{2+} has been reported to exert preventive and ameliorating effects in a rat model of Parkinson's disease based on 1-methyl-4-phenylpyridinium (MPP$^+$) toxicity in dopaminergic neurons.[11] Although Mg^{2+} has been shown to modulate many phenomena in cells, the underlying molecular mechanisms have not been elucidated in detail despite the development of several Mg^{2+} probes.[12] This can partly be attributed to the fact that, in comparison to indicators for Ca^{2+}, many Mg^{2+} indicators designed for use in cells are not sufficiently selective. Therefore, our group has developed the highly selective Mg^{2+} indicator KMG-104.[13] KMG-104 has been used widely and revealed Mg^{2+} mobilization in cytoplasm in various types of cells.[14,15] For detailed understanding of Mg^{2+} mobilization and its mecha-

nisms, however, measuring the changes in Mg^{2+} concentration in specific areas of cells is required. KMG-104 diffuses over the entire cytoplasm and is not appropriate for analyzing the dynamics of intracellular Mg^{2+} around particular proteins, target organelles, and Mg^{2+} transporters or channels.

In the present study, therefore, a novel Mg^{2+} selective fluorescent probe, KMG-104-AsH, was developed by combining KMG-104 and the fluorescent probe for protein-labeling, "FlAsH". FlAsH-type probes are nonfluorescent in the free state and have a high specific affinity in their biarsenical structure for tetracysteine-tagged proteins.[16,17] When the probe binds to the tetracysteine-tag (TCtag) to form the probe–TCtag complex, its fluorescence turns on. However, KMG-104-AsH has a double quenching mechanism: one from the biarsenical–TCtag binding system in the FlAsH substructure, and a second from the Mg^{2+} binding system in KMG-104 substructure. Accordingly, KMG-104-AsH only becomes fluorescent when binding to both the TCtag and Mg^{2+}. Therefore, this probe was shown to be useful for localized molecular imaging of changes in Mg^{2+} concentration.

■ EXPERIMENTAL SECTION

Synthesis and General Procedures. NMR spectra were obtained on JEOL JNM-EXC400, JNM-AL400, and JNM-ALPHA400 spectrometers [[1]H (400 MHz), [13]C (100 MHz)] in a deuteromethanol (CD$_3$OD) solution using CD$_2$HOD as an internal standard and a DMSO-d_6 solution using DMSO$_{5d}$ as an internal standard. High-resolution ESI-mass spectra were obtained on a Waters LCT Premier XE (Waters, Milford MA). HPLC purification was performed on a system consisting of a JASCO PU-2080 Plus pump equipped with a JASCO UVIDEC-100-V detector using a Senshu Pak PEGASIL ODS column (10ϕ × 150 mm) (Senshu Scientific, Tokyo, Japan). The solvents used for HPLC were obtained from Nakalai Tesque (Kyoto, Japan) and filtered through a MILLIPORE OMNIPORE membrane filter (0.45 μm pore size, 47 mm diameter, Millipore, Billerica, MA) before use. Silica gel column chromatography was performed on silica gel 60N (spherical, neutral, 63-210 μm, Kanto Chemical, Tokyo, Japan). Reversed-phase open-column chromatography was performed on PEGASIL PREP ODS-7515-12A (Senshu Scientific). TLC was performed on silica gel plates F$_{254}$ [0.25 mm (analytical) and 0.50 mm (preparative)] (Merck, Tokyo, Japan). 4-Fluororesorcinol was purchased from Sigma-Aldrich (St. Louis, MO).

Synthesis of KMG-104-AsH. *1-(Bis(2,4-dihydroxy-5-fluorophenyl)methyl)-4-oxo-4H-quinolizine-3-carboxylate Ethyl Ester (5).* A stirred solution of ethyl 1-formyl-4-oxo-4*H*-quinolizine-3-carboxylate (compound **4**) (284 mg, 1.16 mmol) and 4-fluororesorcinol (330 mg, 2.58 mmol) in CH$_2$Cl$_2$/Et$_2$O (= 1:1, 6.0 mL) was mixed with methanesulfonic acid (0.48 mL, 8% (v/v) vs solvent) at room temperature under Ar.[18] After the solution was stirred for 17 h, ice-cold water (30 mL) was added into the mixture in an ice bath to give a yellow precipitate, and the supernatant was removed by decantation. The yellow residue was dissolved in MeOH, and the solution was neutralized by Amberlite IRA-400 (OH^{−}) and a small amount of saturated NaHCO$_3$ aq to pH 6−7 and filtered. The filtrate was evaporated in vacuo and purified by silica gel column chromatography (chloroform−methanol = 7:1) to give 531 mg (95%) of compound **5** as a yellow powder.

5: ^{1}H NMR (CD$_3$OD) 9.48 (1H, d, *J* = 6.9 Hz), 7.93 (1H, s), 7.90 (1H, d, *J* = 8.8 Hz), 7.81 (1H, dt, *J* = 1.5, 6.9 Hz), 7.41 (1H, dt, *J* = 1.5, 8.3 Hz), 6.47 (2H, dd, *J* = 2.5, 7.8 Hz), 6.40 (2H, d, *J* = 12.2 Hz), 6.20 (1H, s), 4.27 (2H, q, *J* = 6.8, Hz), 1.29 (3H, t, *J* = 6.8 Hz) ppm; ^{13}C NMR (CD$_3$OD) 167.6, 157.3, 152.1, 147.8, 146.1, 145.5, 145.2, 145.1, 140.7, 136.0, 130.9, 123.9, 120.7, 120.6, 118.8, 118.3, 118.3, 117.3, 117.1, 105.9, 105.1, 61.7, 38.5, 14.6 ppm; HR ESI MS [M][+] found *m/z* 484.1207, C$_{25}$H$_{19}$NO$_7$F$_2$ requires 484.1208.

1-(2,7-Difluoro-6-hydroxy-3-oxo-3H-xanthen-9-yl)-4-oxo-4H-quinolizine-3-carboxylate Ethyl Ester (6, KMG-104 Ethyl Ester). A solution of **5** (141 mg, 0.29 mmol) in methanesulfonic acid (3 mL) was heated to 110 °C for 2 h. After the solution was cooled to 0 °C, cold water (30 mL) was added to give a dark orange solid. The precipitate was filtered and washed twice with water. The filtrate was extracted with EtOAc (30 mL) three times, and the combined organic layer was washed with brine and evaporated in vacuo. The residue was combined with the dark orange precipitate and purified by silica gel chromatography (chloroform−methanol = 5:1 to chloroform−methanol = 5:1 + 0.1% TFA). The dark orange fraction was further purified with a silica gel preparative TLC plate F$_{254}$ (0.50 mm, MERCK) (chloroform−methanol = 4:1 + 0.1% TFA) to give 80.7 mg of **6** (60%) as a bright orange powder.

1-(2,7-Difluoro-6-hydroxy-3-oxo-3H-xanthen-9-yl)-4-oxo-4H-quinolizine-3-carboxylic acid (2, KMG-104). A stirred solution of **6** (29 mg, 0.062 mmol) in H$_2$O/EtOH = 1:1 (2.5 mL) was mixed with 1.0 M LiOH aq (0.25 mL) at 0 °C. The mixture was stirred at room temperature for 1 h, acidified by TFA to pH 5−6, and extracted four times with EtOAc. The organic layer was evaporated in vacuo to give **2** (15.7 mg, 58%), which was used for the next step without further purification.

1-(2,7-Difluoro-6-hydroxy-4,5-bis(trifluoroacetoxymercuri)-3-oxo-3H-xanthen-9-yl)-4-oxo-4H-quinolizine-3-carboxylic Acid (7). A mixture of **2** (51 mg, 0.12 mmol) and HgO (50 mg, 0.23 mmol) in TFA (3.0 mL) was stirred at room temperature overnight and

evaporated in vacuo to give crude **7** (138 mg, quant) as a dark red solid, which was used without further purification.

1-(2,7-Difluoro-6-hydroxy-4,5-bis(1,2,3-dithioarsolan-2-yl)-3-oxo-3H-xanthen-9-yl)-4-oxo-4H-quinolizine-3-carboxylic Acid (1, KMG-104-AsH). A stirred solution of crude **7** (138 mg) in dry NMP (2.0 mL) was carefully mixed with anhydrous diisopropylethylamine (0.40 mL), arsenic trichloride (0.15 mL, 1.76 mmol), and palladium(II) acetate (50 mg, 0.23 mmol) under Ar. After being stirred at room temperature for 18 h, the mixture was poured into 20 mL of 0.5 M potassium phosphate buffer (pH 6.2)/acetone (3:2) to give a dark red solution. After the addition of 1,2-ethanedithiol (0.50 mL) and chloroform (16 mL), the mixture was stirred at room temperature for 30 min. The mixture was diluted with water (30 mL) and extracted with chloroform (15 mL × 3). The organic layers were combined and dried with Na$_2$SO$_4$. After evaporation, the crude product was purified by silica gel chromatography (chloroform−EtOAc = 1:1 + 0.1% TAF to chloroform−EtOAc = 1:3 + 0.1% TAF). The eluted orange fraction was concentrated, triturated with 50% EtOH, and filtered. The obtained pellet was dried overnight on the filter without vacuum[19] to give 15.3 mg (17% in three steps) of the final product **1** as a bright orange powder.

1: ^{1}H NMR (400 MHz, CDCl$_3$−CD$_3$OD (1:1), rt) 9.18 (1H, d, *J* = 7.3 Hz), 8.03 (1H, d, *J* = 1.9 Hz), 7.51 (1H, t, *J* = 7.3 Hz), 7.07 (1H, d, *J* = 9.8 Hz), 6.86 (1H, t, *J* = 7.3 Hz), 6.50 (2H, d, *J* = 10.8 Hz), 3.04 (8H, m) ppm; ^{13}C NMR (100 MHz, DMSO-d_6, rt) 174.8, 166.4, 160.9, 159.3, 159.1, 158.9, 158.6, 157.4, 151.0, 148.6, 144.5, 140.2, 137.5, 130.0, 124.8, 120.1, 119.6, 117.9, 117.3, 114.3, 112.4, 109.4, 105.3, 104.2, 42.7, 42.6 ppm; HR ESI MS (positive) [M][+] found *m/z* 767.8420, C$_{27}$H$_{18}$NO$_6$S$_4$As$_2$F$_2$ requires 767.8417.

Fluorescent Properties of KMG-104-AsH. A 1 mM solution of KMG-104-AsH in DMSO was prepared, and 1 μL was added into 1 mL of 10 mM MOPS/KOH (pH 7.3) buffer containing 100 mM KCl, 10 mM MESNa, 3 mM TCEP, 10 μM EDT, MgCl$_2$, CaCl$_2$, or other ions at varying concentrations, and TCtag peptide (Ac-FLNCCPGCCMEP) (0 or 1 μM in 50% acetonitrile containing 0.1% TFA). Custom TCtag peptide and its analogues were purchased from Toray Research Center. Absorbance spectra were recorded on a U-2001 spectrophotometer (HITACH) using quartz cuvettes. Fluorescence spectra were recorded in a F-4500 fluorophotometer (HITACHI) using quartz cuvettes. The excitation wavelength was set to 505 nm.

Determination of the Apparent Dissociation Constant. The apparent dissociation constant (K_d) of the KMG-104-AsH-TCtag complex for Mg^{2+} was calculated as 1.7 mM. To determine the K_d, the Benesi−Hildebrand plot method was used. The increase in fluorescence intensity ($I - I_0$) was measured and fitted to the following equation

$$1/(I - I_0) = 1/(A[\text{probe} - \text{tag complex}])$$
$$+ 1/(AK_d[\text{probe} - \text{tag complex}]) \times 1/([\text{Mg}^{2+}])$$

where I is the measured fluorescence intensity, I_0 is the fluorescence intensity at 0 mM of Mg^{2+}, and A is a constant. Plotting $1/(I - I_0)$ and $1/([\text{Mg}^{2+}])$, K_d was obtained from the value of (y-intercept)/(slope) using an approximate line. Fluorescence intensities for the calculation of K_d are shown in Figure 3.

Gene Construction. The DNA sequence encoding the TCtag peptide (FLNCCPGCCMEP) was fused to the N′-terminus of actin by polymerase chain reaction (PCR). The PCR product was sequenced to ensure fidelity and subcloned into a pcDNA3.1(+) vector (Invitrogen, Carlsbad, CA) at the *Kpn*I and EcoR I restriction enzyme sites. mKeima was purchased from Amalgaam (Tokyo, Japan), and its C′-terminus was fused to the TCtag sequence. To localize mKeima−TCtag to the MIS, a MIS localization signal was also conjugated to the N′-terminus of mKeima−TCtag. MIS targeted mKeima−TCtag was inserted into the pEGFP-N1 vector (Clontech, Mountain View, CA), exchanging for EGFP, between the EcoR I and Not I restriction enzyme sites, and mKeima−TCtag was inserted between the BamH I and Not I sites. The recombinant plasmids were
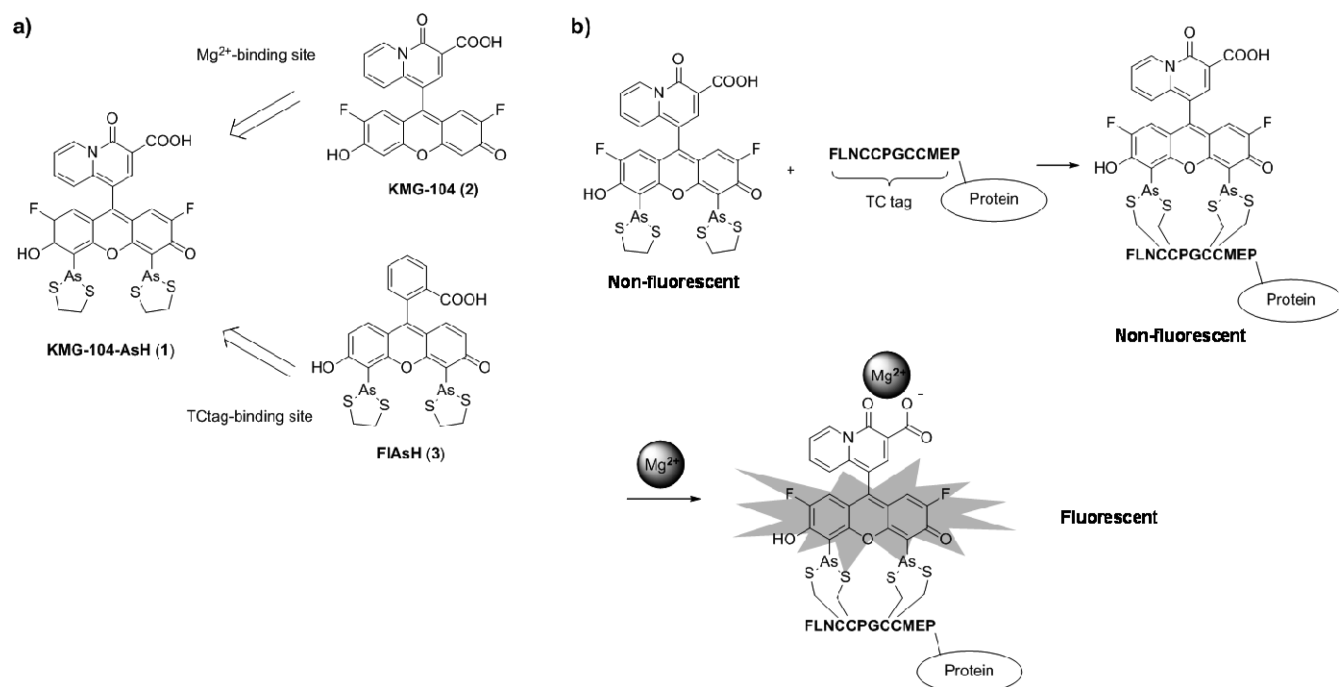
Figure 1. Molecular design of KMG-104-AsH: (a) KMG-104-AsH (**1**) was derived from KMG-104 (**2**), a highly selective Mg^{2+} probe, and FlAsH (**3**), a fluorescent probe that specifically binds to a tetra-cysteine peptide tag (TCtag). (b) KMG-104-AsH only emits fluorescence when bound to both the TCtag and Mg^{2+}. KMG-104-AsH allows for the detection of local changes in Mg^{2+} concentration around any protein genetically modified to express the TCtag.

amplified in *Escherichia coli* DH5α (Toyobo, Tokyo, Japan) and purified using a Qiagen plasmid maxi kit (Qiagen, Tokyo, Japan).

Cell Culture and Transient Transfection. HeLa cells were cultured in DMEM supplemented with 10% FBS and 1% penicillin/streptomycin (Invitrogen) in an incubator maintained at 37 °C and a humidified atmosphere of 5% CO_2. For experimental use, cells were seeded onto glass-based dishes (Iwaki, Tokyo, Japan). Each amplified plasmid (2 μg for each dish) was transfected into the HeLa cells with the Lipofectamine LTX and Plus reagent (Invitrogen). Experiments were performed 24 h after transfection.

Fluorescence Measurements Using Confocal Scanning Microscopy. KMG-104-AsH was stored at −20 °C as a 1 mM stock solution in DMSO. Transfected HeLa cells were incubated at 37 °C for 1 h with 100 μL of HBSS (buffered to pH7.3 by 10 mM HEPES) containing 1 μM KMG-104-AsH and 10 μM EDT. The cells were incubated twice for 10 min in HBSS containing 250 μM EDT to wash out the excess probe binding to peptide sequences other than TCtag. After the washing solution was removed, the dish was filled with HBSS, and cells were visualized with a confocal laser scanning microscope (FV-1000, Olympus, Tokyo, Japan) equipped with a 60× oil immersion objective lens (Olympus) and a DM405-440/515 dichroic mirror (Olympus). Fluorescence was measured with a photomultiplier (Olympus). KMG-104-AsH was excited by an Ar laser (515 nm). For simultaneous measurements of KMG-104-AsH and mKeima, these probes were excited at 515 nm (with the Ar laser) and at 440 nm (with the laser diode), respectively. The signals were separated with a 600 nm dichroic mirror and detected 530−550 nm (for KMG-104-AsH) and 630−730 nm (for mKeima) using monochromaters.

Time-lapse imaging of the responses to the FCCP stimulus was carried out for the above stained cells. FCCP solution was added to bring the final concentration to 5 μM, and the change in fluorescence intensity was recorded.
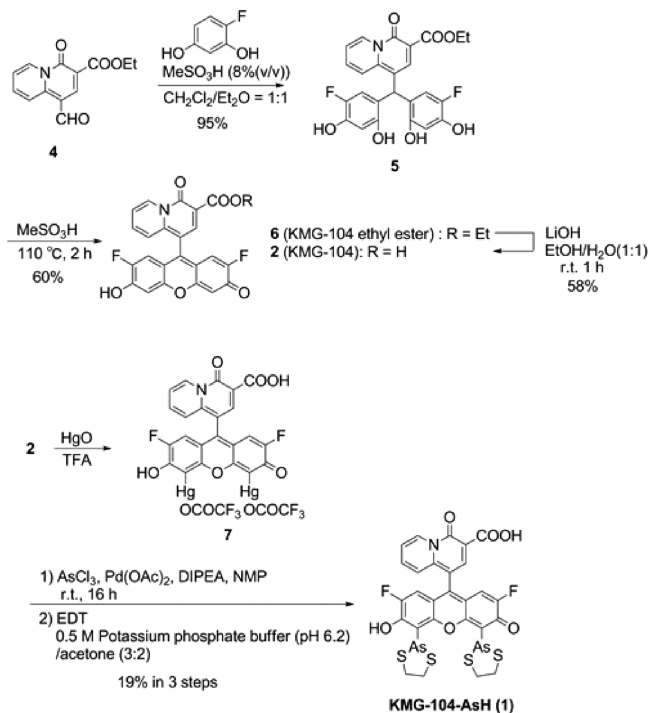
■ RESULTS

Molecular Design. KMG-104 is a Mg^{2+}-selective indicator showing a fluorescence increase behavior upon binding of Mg^{2+}

to the charged β-diketone site[20,21] in the quinolidine derivative moiety. In its unbound state, the fluorescence emission is quenched by photoinduced electron transfer (PET).[22−25] The FlAsH probe is also quenched in its unbound state, presumably by vibrational deactivation or PET mechanisms,[17] and becomes fluorescent when specifically binding to the tetracysteine peptide sequence (TCtag; amino acid sequence: FLNCCPGCCMEP) due to the formation of a rigid and constrained peptide complex.[16,17,26] We focused our attention on the xanthene fluorophore system, which is the molecular subunit common to both of these fluorescent probes. It was hypothesized that by attaching the Mg^{2+}-binding moiety of KMG-104, 4-oxo-4H-quinolizine-3-carboxylic acid, to the 9-position of 2,7-difluoro-4,5-bis(1,2,3-dithioarsolan-2-yl)-xanthene in FlAsH, a new Mg^{2+} probe possessing the functions of both KMG-104 and FlAsH would be obtained (Figure 1a). This novel Mg^{2+} probe "KMG-104-AsH" was designed to emit bright fluorescence only when bound to both Mg^{2+} and the TCtag. This unique property is due to the independent fluorescence quenching mechanisms at the Mg^{2+}-binding site (PET-type response) and at the arsenic atoms (free rotation).[16] While the FlAsH-type probe is activated upon binding to the TCtag peptide sequence, KMG-104-AsH remains quenched by a PET mechanism in the KMG-104 substructure in the absence of Mg^{2+}. Conversely, without binding to the TCtag peptide, KMG-104-AsH remains in its turned-off state even in the presence of sufficient Mg^{2+}. The TCtag is a small peptide tag that can be genetically fused to any protein and expressed transiently in cells. KMG-104-AsH is expected to act as selectively as KMG-104 for the detailed detection of Mg^{2+} dynamics, and as specifically as FlAsH for the detection of proteins containing the TCtag (Figure 1b). Because these combined functionalities could be of value for elucidating the

molecular mechanisms of Mg^{2+} mobilization, KMG-104-AsH was synthesized and its properties were analyzed.

Synthesis of the KMG-104-AsH. The novel Mg^{2+} fluorescent probe "KMG-104-AsH" (**1**) was synthesized as shown in Scheme 1. The quinolizine derivative **4**, which was
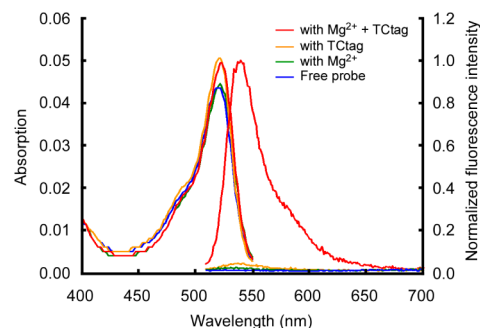
Scheme 1. Organic Synthesis of KMG-104-AsH

Figure 2. Absorption and fluorescence emission spectra of KMG-104-AsH (1 μM) in the absence or presence of Mg^{2+} ($[Mg^{2+}]$ = 0 or 100 mM) and of the TC tag peptide (Ac-FLNCCPGCCMEP, 0 μM or 4 μM). All spectra were measured at pH 7.3 (10 mM MOPS buffer, 100 mM KCl, 10 mM MESNa, 3 mM TCEP, 10 μM EDT). For the measurement of emission spectra, KMG-104-AsH was excited at 505 nm.

S1, Supporting Information). In the absence of the TCtag peptide, there was only a slight increase in the maximum fluorescence intensity of KMG-104-AsH when the Mg^{2+} ion concentration was increased from 0 to 100 mM. In contrast, the addition of 4 μM TCtag peptide induced a more than 10-fold increase of the maximum fluorescence intensity dependent on the Mg^{2+} concentration. These results suggest that the fluorescence intensity of KMG-104-AsH increased only upon binding of the probe molecule to both the TCtag peptide and Mg^{2+}, as was expected from the design of the molecule. The $K_{d/Mg}$ value of KMG-104-AsH was calculated to be 1.7 mM, which is similar to KMG-104 (2.1 mM).[13]

The selective binding affinity of KMG-104-AsH for Mg^{2+} compared to Ca^{2+}, which is another abundant divalent cation in cells, was investigated and compared (Figure 3a). No changes in fluorescence intensity were observed in the presence of Ca^{2+} concentrations in the range of 0.1−100 mM. The dissociation constant of KMG-104-AsH for Ca^{2+} ($K_{d/Ca}$) was estimated to be above 100 mM, which is significantly higher than $K_{d/Mg}$ of 1.7 mM. Other cations, such as Na^+, K^+, Ni^{2+}, Mn^{2+}, Co^{2+}, Zn^{2+}, Fe^{2+}, Cu^{2+} and Cu^+, also had no effect on the fluorescence of KMG-104-AsH and on the Mg^{2+} binding ability of KMG-104-AsH in the concentration range based on physiological environment (Figure 3b and Figure S1,Supporting Information) as well as pH (5.5−8) (Figure 4). The pK_a value of this probe was calculated to be 4.2 in 0.1 M acetic acid buffer containing TCtag and 100 mM Mg^{2+} (Figure S2, Supporting Information). Moreover, in the presence of TCtag analogues with one or more cysteine residues in the peptide tag replaced by alanine, KMG-104-AsH showed only slight Mg^{2+} concentration-dependent fluorescence intensity changes in the presence of 250 μM EDT (Figure 5). Although KMG-104-AsH bound to TCtag analogues in the buffer containing 10 μM EDT, 250 μM EDT, which was used for washing out KMG-104-AsH in the cell-staining procedure, was sufficient to dissociate KMG-104-AsH from peptide sequences other than TCtag sequence (Figure S3, Supporting Information). The same EDT concentration (250 μM) was also suitable for the staining of cells withKMG-104-AsH. At lower EDT concentration, the background fluorescence was higher. On the other hand, at higher EDT concentration, KMG-104-AsH was

prepared as described previously,[20] was used as the starting material. Compound **4** was treated with commercially available 4-fluororesorcinol in the presence of 8% (v/v) catalytic methanesulfonic acid[18] to trigger the Friedel−Crafts reaction leading to compound **5**. Initial attempts to synthesize KMG-104 ethyl ester (**6**) by oxidative cyclization of **5** with DDQ in AcOH/benzene[18] were unsuccessful. Therefore, purified **5** was treated with neat methanesulfonic acid at 110 °C yielding KMG-104 ethyl ester (**6**) by the desired dehydrative cyclization.[13,27,28] During purification by silica gel column chromatography and preparative TLC to obtain pure **6**, no cyclic intermediates were detected, indicating that oxidation was prevented. In the next step, KMG-104 (**2**) was obtained by hydrolysis of **6** with 0.25 M LiOH at room temperature for 1 h. This synthetic process resulted in an overall yield of KMG-104 of 33%, which is superior to the 5.8% overall yield reported previously.[13] In addition, the mercuration of KMG-104 was accomplished with mercuric trifluoroacetate, prepared by HgO addition into TFA.[19,29,30] After excess TFA was removed in vacuo, crude mercuric KMG-104 (**7**) was treated in one pot with arsenic trichloride and then 1,2-ethanedithiol (EDT) to yield the biarsenic compound KMG-104-AsH (**1**). The purification of **1** required the trituration of the product after column chromatography, instead of drying in a vacuum line, to prevent the potential decrease of purity caused by the removal of EDT from the arsenic groups and polymerization.[19] Finally, KMG-104-AsH (**1**) was obtained as an orange powder.

Properties of KMG-104-AsH. Although the absorption spectra of KMG-104-AsH did not show significant spectral shifts or changes in absorbance, drastic changes in fluorescence
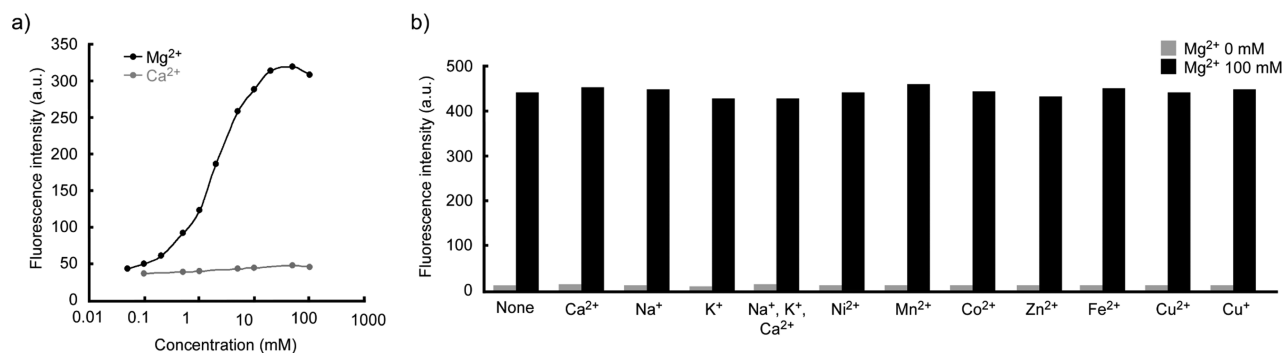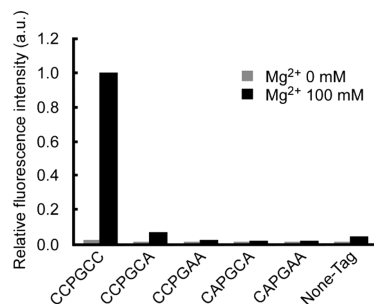
Figure 3. Ion selectivity of KMG-104-AsH: selectivity of KMG-104-AsH for Mg^{2+} compared to Ca^{2+}. (a) Fluorescence intensities of KMG-104-AsH (1 μM) with TCtag (4 μM) at 540 nm (excitation at 490 nm) were measured in the presence of Ca^{2+} or Mg^{2+} at concentrations ranging from 0.1 to 100 mM. (b) Fluorescence intensities of KMG-104-AsH binding to TCtag with (black bar) or without (gray bar) 100 mM Mg^{2+} were measured in the presence of Ca^{2+} (1 mM), Na^+ (10 mM), K^+ (100 mM), Ni^{2+}, Mn^{2+}, Co^{2+}, Zn^{2+}, Fe^{2+}, Cu^{2+}, or Cu^+ (1 μM). Cu^+ was reduced from Cu^{2+} by addition of 100 equiv of ascorbic acid relative to the Cu^{2+} concentration. The concentrations of those ions were chosen according to the physiological concentrations. All measurements were performed in 10 mM MOPS buffer at pH 7.3.
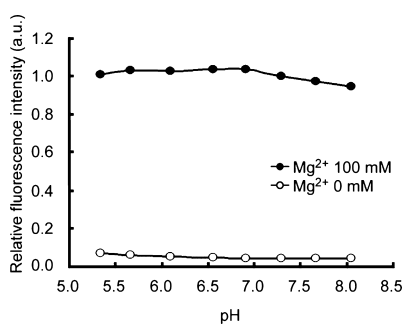
Figure 4. Effect of pH on the fluorescence intensity of KMG-104-AsH bound to the TCtag: Probe and tag peptide were prepared in buffer at pH 5.5−6.5 (10 mM MES) and pH 7.0−8.0 (10 mM MOPS) and then mixed with MOPS buffer with or without Mg^{2+}. The final pH values are shown on the horizontal axis, and those of KMG-104-Ash and TCtag peptide are 1 and 4 μM, respectively. The fluorescence intensities were normalized to the value at pH 7.3 with 100 mM of Mg^{2+}.


Figure 5. Selectivity for the TCtag: fluorescence intensities of KMG-104-AsH in the presence of the TCtag or other similar peptide sequences (TCtag analogues) were compared in MOPS buffer (pH 7.3) containing EDT 250 μM. In the analogue peptide sequences, the KMG-104-AsH binding sequence (CCPGCC) in the TCtag peptide sequence (FLNCCPGCCMEP) was replaced by the peptide sequences shown.

removed from the TCtag sequence (Figure S4, Supporting Information). The selective recognition of the simultaneous presence of Mg^{2+} and the TCtag by KMG-104-AsH indicates that the binding affinities for Mg^{2+} and for the TCtag peptide of the KMG-104 and FlAsH probes have been retained.

It was also demonstrated that the concentration of KMG-104-AsH applied for cellular staining is not detrimental to cell viability (Figure S5, Supporting Information). These results clearly indicate that KMG-104-AsH is a suitable probe for live cell imaging.

Application of KMG-104-AsH to Cultured Cells. KMG-104-AsH was applied to fluorescence imaging in cultured HeLa cells expressing TCtag-labeled proteins. As shown in Figure 6a, the TC-tagged actins were clearly stained with KMG-104-AsH, indicating the formation of a KMG-104-AsH−TCtag−-Mg^{2+} complex in the intracellular environment. These results also demonstrated the permeability of the cell membrane to KMG-104-AsH without acetoxymethylation of the carboxyl group. The intracellular localization of KMG-104-AsH was comparable
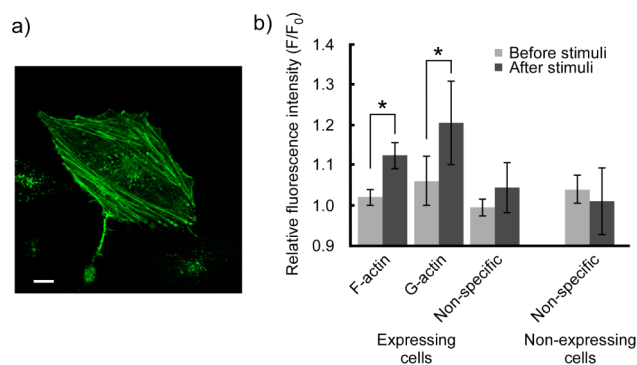

Figure 6. Application to live cell imaging. (a) Fluorescence image of HeLa cells stained with KMG-104-AsH, expressing TCtag-actin. Intensive fluorescence on actin filaments (F-actin), weak fluorescence in the cytoplasm, in which tagged G-actin might bind to KMG-104-AsH (G-actin), and granular fluorescence, which correspond to the distribution of actin (Nonspecific), were observed. The nonspecific fluorescence was often observed in cells not expressing TCtag-actin. The scale bar represents 20 μm. (b) Fluorescence intensities of KMG-104-AsH were normalized to the initial value and compared before and after FCCP treatment of various areas in HeLa cells ($n = 5$). On F-actin and G-actin, KMG-104-AsH showed increased fluorescence after administration of FCCP. On the other hand, no changes in the fluorescence upon nonspecific staining were detected in TCtag-actin expressing and nonexpressing cells. Averaged fluorescence intensities measured for 1 min before stimulation and from 1 to 2 min after stimulation were compared. Error bars indicate the standard error of the mean (*$P < 0.05$ in Student's t test).

to that of the commercially available FlAsH in TCtag—actin expressing HeLa cells (Figure S6, Supporting Information).[26] Both of those stained actins polymerized in filamentous form (F-actin) and monomer actins (G-actin). In KMG-104-AsH-loaded cells, granular fluorescence was also observed both in TCtag expressing and nonexpresssing cells, which could be attributed to the partial uptake of KMG-104-AsH into intracellular compartments such as the endosome and lysosome. Nevertheless, this nonspecific fluorescence did not change in intensity in response to changes in Mg^{2+} concentration in the cytoplasm (Figure 6b). These results demonstrated that changes in the fluorescence intensity of KMG-104-AsH occur only when it is bound to the TCtag, and the nonspecific TCtag-independent accumulation of KMG-104-AsH does not affect the measurements of intracellular Mg^{2+} levels.

Next, the changes in Mg^{2+} concentration in the cytoplasm and around mitochondria were compared. To eliminate the effects of mitochondrial movement, the monomeric red fluorescent protein mKeima was used as a reference. To examine the Mg^{2+} sensitivity of KMG-104-AsH bound to tagged protein in the intracellular environment, the cell membrane was rendered permeable with digitonin,[29] and fluorescence ratios of KMG-104-AsH to mKeima were measured at various Mg^{2+} concentrations (Figure S7, Supporting Information). The K_d value was calculated to be 5.7 mM. Although this value is slightly higher than the one found in MOPS buffer solution (1.7 mM), it is suitable to measure the changes in intracellular Mg^{2+} concentrations. Similar differences in K_d values measured in the intracellular environment and in solution were also observed for Ca^{2+} in the case of Calcium Green FlAsH.[29] To localize the mKeima—TCtag to the proximal region of the mitochondrial matrix, a mitochondrial intermembrane space (MIS) localization signal[31] was added to the N′-terminus of mKeima (Figure 7a). While the mKeima—TCtag localized to the cytoplasm, the MIS-targeted mKeima—TCtag localized to mitochondria (Figure 7b). The localization of KMG-104-AsH overlapped with the distribution of the mKeima—TCtag. The time-courses of the Mg^{2+} concentration changes in the cytoplasm and the MIS were compared. Carbonyl cyanide p-(trifluoromethoxy) phenylhydrazone (FCCP) initially induced a steep increase in the Mg^{2+} concentration in the MIS, followed by a gradual increase in cytoplasmic Mg^{2+} concentration (Figure 7c), indicating the diffusion of Mg^{2+} from the mitochondria to the cytoplasm in HeLa cells. No photobleaching was observed for KMG-104-AsH during time-laps imaging of less than 10 min (Figure S8, Supporting Information).

■ DISCUSSION

Although Mg^{2+} plays critical roles in a number of physiological processes, a clear understanding of the molecular mechanisms underlying the cellular functions of Mg^{2+} has been hampered by the lack of reliable probes for use in cell experiments. The classical Mg^{2+} probes such as mag-fura-2 and magnesium-green have a limited ability for distinguishing between signals originating from Mg^{2+} or Ca^{2+} because of their relatively low dissociation constant for Ca^{2+} ($K_{d/Ca}$) compared to that for Mg^{2+} ($K_{d/Mg}$).[32,33] KMG series dyes were developed as highly selective intracellular free Mg^{2+} probes with an adequate $K_{d/Mg}$ for the detection of Mg^{2+} within the intracellular concentration range, without responding to Ca^{2+}.[13,21,34] KMG-104 was shown to be effective for detecting changes in the concentration of
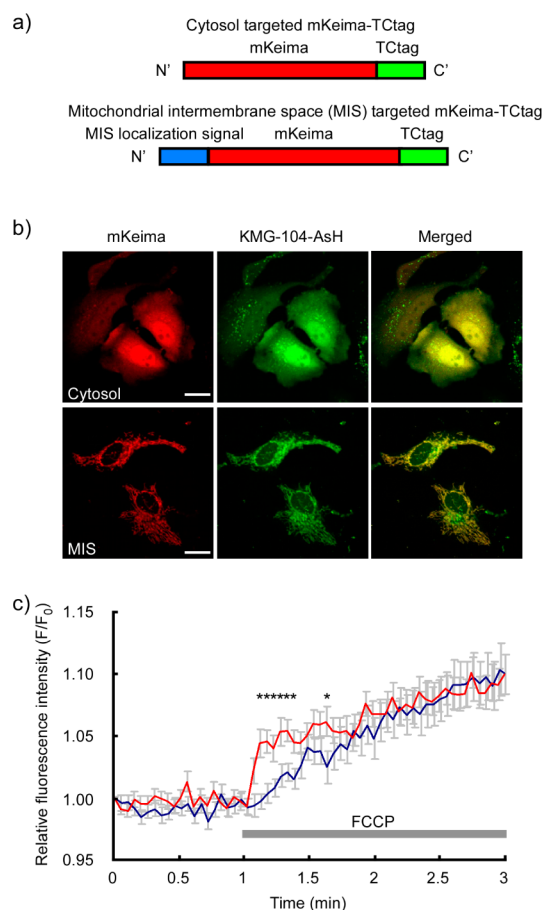
Figure 7. Mg^{2+} imaging in localized intracellular regions. (a) Design of mKeima-TCtag and mKeima-TCtag with a mitochondrial intermembrane space (MIS) localization signal. (b) Fluorescence images of cytoplasmic and MIS-targeted mKeima-TCtag. mKeima-TCtag was detected as a diffuse pattern in the cytoplasm, whereas MIS targeted mKeima-TCtag localized to mitochondria (red). The fluorescence of KMG-104-AsH overlapped with the distribution of mKeima-TCtag (green and merged). The scale bar indicates 20 μm. (c) Time-courses of Mg^{2+} concentration in the cytoplasm (blue, n = 19) and the MIS (red, n = 29). The ratio of the fluorescence of KMG-104-AsH to that of mKeima was normalized to the initial value. Error bars indicate the standard error mean (*P < 0.05 in Student's t test).

Mg^{2+} in the whole cytoplasm and used to demonstrate Mg^{2+} mobilizations.[35−37] In resent years, other groups also developed unique Mg^{2+}-selective fluorescent probes, such as a Mg^{2+} probe suitable for two-photon microscopy, and detected intracellular Mg^{2+} concentration changes.[12,38,39] To clarify the mechanisms and roles underlying intracellular Mg^{2+} concentration changes, however, a novel type of probe for monitoring the concentration changes in particular regions in cells is required. In this study, KMG-104-AsH was developed by combining a Mg^{2+}-selective probe, KMG-104, and a fluorescent probe for protein-labeling, FlAsH. KMG-104-AsH maintains the Mg^{2+} selectivity and the pH insensitivity of KMG-104 (Figures 3 and 4) and binds specifically to the TCtag peptide sequence similar to FlAsH (Figure 5). It had no toxicity to cells when used at concentrations relevant for staining (Figure S5, Supporting Information). Therefore, we concluded that KMG-104-AsH is an effective probe for measuring local changes in Mg^{2+} concentration around tagged proteins. In a previous study, the Ca^{2+} indicator Calcium green was conjugated to FlAsH, and

local Ca^{2+} dynamics around gap junctions in HeLa cells were observed and analyzed.[29] In this study, by conjugating KMG-104 to FlAsH, a novel tool for visualizing intracellular local dynamics of another essential divalent cation, Mg^{2+}, has been developed. These probes are expected to be powerful tools for the detailed elucidation of cellular events.

KMG-104-AsH was successfully used to visualize actin filaments transfected with TCtag peptides in HeLa cells (Figure 6a). The results indicated that KMG-104-AsH was sufficiently membrane-permeable without acetoxymethylation of the carboxyl group in the quinolizine derivative moiety, which is necessary for loading KMG-104 into cells, and showed specific intracellular binding to TCtag, similar to FlAsH. Depending on the localization of tagged proteins, localization of KMG-104-AsH to specific areas in cells was enabled. This allows to measure changes in Mg^{2+} concentration in specific local regions in cells. Therefore, TCtagged mKeima was localized to the region proximal to the mitochondrial matrix, since the release of Mg^{2+} from mitochondria upon depolarization of their inner membrane potential was demonstrated in our previous studies.[35,36] Membrane depolarization caused a sharp increase in Ca^{2+} concentration followed by a gradual increase in Mg^{2+} concentration in the cytoplasm of PC12 cells. However, the concentration of Mg^{2+} in a small region around the mitochondrial matrix might show sharper changes than in the cytoplasm. Therefore, to test this hypothesis, a localization signal sequence specific for the MIS was attached to the N′-terminus of the mKeima−TCtag, and the change in Mg^{2+} levels in the region proximal to the mitochondrial matrix was measured. As shown in Figure 7c, Mg^{2+} levels showed an initial steep increase in the MIS followed by a gradual increase in the cytoplasm, indicating the diffusion of Mg^{2+} from the mitochondrial matrix to the cytoplasm. In addition, the combined use of KMG-104-AsH with mKeima enables to eliminate the effects of movements of cells and organelles by calculating the changes in relative fluorescence intensity of KMG-104-AsH in reference to that of mKeima. Moreover, the fluorescence ratio of KMG-104-AsH to mKeima correlated with the intracellular Mg^{2+} concentration (Figure S7, Supporting Information). Using this method, it was estimated that FCCP induced an increase in Mg^{2+} concentration in the cytoplasm in HeLa cells from 0.5 mM to 1.1 mM (Figure S9, Supporting Information). These values are consistent with the Mg^{2+} concentration ranges evaluated with other methods,[40] indicating that KMG-104-AsH allows quantitative measurements. These are advantages of this method over KMG-104 and other nonratiometric probes.

In this work, the TCtag-selective Mg^{2+} fluorescent probe, KMG-104-AsH, was synthesized and applied to Mg^{2+} imaging in local regions in HeLa cells. Changes in Mg^{2+} concentration around mitochondria have been associated with apoptosis.[41] It indicates the possibility that imaging of Mg^{2+} concentration in the local region around mitochondria reveals the contribution of Mg^{2+} as an intracellular signal to mitochondria. Moreover, a recent study revealed that Mg^{2+} influx via the selective Mg^{2+} channels MagT1 and TUSC3 is required for embryonic development in zebrafish[14] and that via MagT1 also acts as a second messenger in T cells.[42] These findings suggest that changes in Mg^{2+} concentration around organelles and specific proteins may play important roles in cellular processes. The bifunctional KMG-104-AsH probe developed in this work is expected to be a strong tool for the elucidation of the little-known molecular mechanisms and critical roles of Mg^{2+} in cells.

CONCLUSION

To detect and image the local change in concentration of Mg^{2+} in cells, the novel fluorescence Mg^{2+} selective probe, KMG-104-AsH, was designed and synthesized. It was derived from the highly selective Mg^{2+} probe, KMG-104, and the FlAsH probe that fluoresces only when it binds specifically to a TCtag peptide genetically added to target proteins. We showed that the probe has effective fluorescence properties, in that its fluorescence increases drastically when it binds to both Mg^{2+} and TCtag. This effect results from the cancellation of a PET effect and free rotations of arsenic groups. KMG-104-AsH was also shown to be membrane-permeable, and it stains TC-tagged actins and TC-tagged mKeima localized to the mitochondrial intermembrane space in HeLa cells. We succeeded in detecting the change in Mg^{2+} concentration induced by FCCP around TC-tagged proteins. This probe is expected to be a strong tool for the elucidation of little known molecular mechanisms and critical roles of Mg^{2+} in cells.

ASSOCIATED CONTENT

Ⓢ Supporting Information

Supproting figures. This material is available free of charge via the Internet at http://pubs.acs.org.

AUTHOR INFORMATION

Corresponding Author
oka@bio.keio.ac.jp

Author Contributions
⊥These authors contributed equally to this work.

Notes
The authors declare no competing financial interest.

ACKNOWLEDGMENTS

REFERENCES

(1) Matsuda, H.; Saigusa, A.; Irisawa, H. *Nature* **1987**, *325*, 156−9.
(2) Romani, A. M.; Scarpa, A. *Front Biosci.* **2000**, *5*, D720−34.
(3) Politi, H. C.; Preston, R. R. *Neuroreport* **2003**, *14*, 659−68.
(4) Gwanyanya, A.; Amuzescu, B.; Zakharov, S. I.; Macianskiene, R.; Sipido, K. R.; Bolotina, V. M.; Vereecke, J.; Mubagwa, K. *J. Physiol.* **2004**, *559*, 761−76.
(5) Rodriguez-Zavala, J. S.; Moreno-Sanchez, R. *J. Biol. Chem.* **1998**, *273*, 7850−5.
(6) Boska, M. D.; Welch, K. M.; Barker, P. B.; Nelson, J. A.; Schultz, L. *Neurology* **2002**, *58*, 1227−33.
(7) Yasui, M.; Kihira, T.; Ota, K. *Neurotoxicology* **1992**, *13*, 593−600.
(8) Keenan, D.; Romani, A.; Scarpa, A. *FEBS Lett.* **1996**, *395*, 241−4.
(9) Touyz, R.; Mercure, C.; Reudelhuber, T. *Mol. Aspects Med.* **2003**, *24*, 107−136.
(10) Sontia, B.; Touyz, R. M. *Arch. Biochem. Biophys.* **2007**, *458*, 33−9.
(11) Hashimoto, T.; Nishi, K.; Nagasao, J.; Tsuji, S.; Oyanagi, K. *Brain Res.* **2008**, *1197*, 143−51.
(12) Trapani, V.; Farruggia, G.; Marraccini, C.; Iotti, S.; Cittadini, A.; Wolf, F. I. *Analyst* **2010**, *135*, 1855−66.
(13) Komatsu, H.; Iwasawa, N.; Citterio, D.; Suzuki, Y.; Kubota, T.; Tokuno, K.; Kitamura, Y.; Oka, K.; Suzuki, K. *J. Am. Chem. Soc.* **2004**, *126*, 16353−60.

(14) Zhou, H.; Clapham, D. E. *Proc. Natl. Acad. Sci. U.S.A.* **2009**, *106*, 15750−5.

(15) Jin, J.; Desai, B. N.; Navarro, B.; Donovan, A.; Andrews, N. C.; Clapham, D. E. *Science* **2008**, *322*, 756−60.

(16) Griffin, B. A.; Adams, S. R.; Tsien, R. Y. *Science* **1998**, *281*, 269−72.

(17) Adams, S. R.; Campbell, R. E.; Gross, L. A.; Martin, B. R.; Walkup, G. K.; Yao, Y.; Llopis, J.; Tsien, R. Y. *J. Am. Chem. Soc.* **2002**, *124*, 6063−76.

(18) Bacci, J. P.; Kearney, A. M.; Van Vranken, D. L. *J. Org. Chem.* **2005**, *70*, 9051−3.

(19) Adams, S. R.; Tsien, R. Y. *Nat. Protoc.* **2008**, *3*, 1527−34.

(20) Otten, P. A.; London, R. E.; Levy, L. A. *Bioconjugate Chem.* **2001**, *12*, 203−12.

(21) Suzuki, Y.; Komatsu, H.; Ikeda, T.; Saito, N.; Araki, S.; Citterio, D.; Hisamoto, D.; Kitamura, Y.; Kubota, T.; Nakagawa, J.; Oka, K.; Suzuki, K. *Anal. Chem.* **2002**, *74*, 1423−8.

(22) de Silva, A. P.; Gunaratne, H. Q.; Gunnlaugsson, T.; Huxley, A. J.; McCoy, C. P.; Rademacher, J. T.; Rice, T. E. *Chem. Rev.* **1997**, *97*, 1515−1566.

(23) Nagano, T.; Yoshimura, T. *Chem. Rev.* **2002**, *102*, 1235−70.

(24) Hirano, T.; Kikuchi, K.; Urano, Y.; Higuchi, T.; Nagano, T. *Angew. Chem., Int. Ed.* **2000**, *39*, 1052−1054.

(25) Urano, Y.; Kamiya, M.; Kanda, K.; Ueno, T.; Hirose, K.; Nagano, T. *J. Am. Chem. Soc.* **2005**, *127*, 4888−94.

(26) Martin, B. R.; Giepmans, B. N.; Adams, S. R.; Tsien, R. Y. *Nat. Biotechnol.* **2005**, *23*, 1308−14.

(27) Mottram, L. F.; Maddox, E.; Schwab, M.; Beaufils, F.; Peterson, B. R. *Org. Lett.* **2007**, *9*, 3741−4.

(28) Areephong, J.; Ruangsupapichart, N.; Thongpanchang, T. *Tetrahedron Lett.* **2004**, *45*, 3067−3070.

(29) Tour, O.; Adams, S. R.; Kerr, R. A.; Meijer, R. M.; Sejnowski, T. J.; Tsien, R. W.; Tsien, R. Y. *Nat. Chem. Biol.* **2007**, *3*, 423−31.

(30) Spagnuolo, C. C.; Vermeij, R. J.; Jares-Erijman, E. A. *J. Am. Chem. Soc.* **2006**, *128*, 12040−1.

(31) Ozawa, T.; Natori, Y.; Sako, Y.; Kuroiwa, H.; Kuroiwa, T.; Umezawa, Y. *ACS Chem. Biol.* **2007**, *2*, 176−86.

(32) Brocard, J. B.; Rajdev, S.; Reynolds, I. J. *Neuron* **1993**, *11*, 751−7.

(33) Leyssens, A.; Nowicky, A. V.; Patterson, L.; Crompton, M.; Duchen, M. R. *J. Physiol.* **1996**, *496*, 111−28.

(34) Shindo, Y.; Fujii, T.; Komatsu, H.; Citterio, D.; Hotta, K.; Suzuki, K.; Oka, K. *PLoS One* **2011**, *6*, e23684.

(35) Kubota, T.; Shindo, Y.; Tokuno, K.; Komatsu, H.; Ogawa, H.; Kudo, S.; Kitamura, Y.; Suzuki, K.; Oka, K. *Biochim. Biophys. Acta* **2005**, *1744*, 19−28.

(36) Shindo, Y.; Fujimoto, A.; Hotta, K.; Suzuki, K.; Oka, K. *J. Neurosci. Res.* **2010**, *88*, 3125−32.

(37) Yamanaka, R.; Shindo, Y.; Hotta, K.; Suzuki, K.; Oka, K. *FEBS Lett.* **2013**, *587*, 2643−8.

(38) Dong, X.; Han, J. H.; Heo, C. H.; Kim, H. M.; Liu, Z.; Cho, B. R. *Anal. Chem.* **2012**, *84*, 8110−3.

(39) Kim, H. M.; Jung, C.; Kim, B. R.; Jung, S. Y.; Hong, J. H.; Ko, Y. G.; Lee, K. J.; Cho, B. R. *Angew. Chem., Int. Ed.* **2007**, *46*, 3460−3.

(40) Romani, A. M. *Arch. Biochem. Biophys.* **2011**, *512*, 1−23.

(41) Wolf, F. I.; Trapani, V. *Clin. Sci. (London)* **2008**, *114*, 27−35.

(42) Li, F. Y.; Chaigne-Delalande, B.; Kanellopoulou, C.; Davis, J. C.; Matthews, H. F.; Douek, D. C.; Cohen, J. I.; Uzel, G.; Su, H. C.; Lenardo, M. J. *Nature* **2011**, *475*, 471−6.